Atmospheric Environment 44 (2010) 1152–1161

Contents lists available at ScienceDirect

Atmospheric Environment

journal homepage: www.elsevier.com/locate/atmosenv

Aerosol load study in urban area by Lidar and numerical model

A. Miffre [a], M. Abou Chacra [a], S. Geffroy [a], P. Rairoux [a,*], L. Soulhac [b], R.J. Perkins [b], E. Frejafon [c]

[a] Université Lyon 1, LASIM, CNRS UMR 5579, F-69622 Villeurbanne cedex, France
[b] Laboratoire de Mécanique des Fluides et d'Acoustique, CNRS UMR 5509 Université de Lyon, Ecole Centrale de Lyon, F-69134 Ecully cedex, France
[c] Institut National de l'Environnement Industriel et des Risques, F-60550 Verneuil en Halatte, France

ARTICLE INFO

Article history:
Received 1 August 2009
Received in revised form
18 December 2009
Accepted 23 December 2009

Keywords:
Urban aerosol
UBL
PM10
Lidar
Numerical model

ABSTRACT

Vertical profiles of particle mass concentration in the urban canopy above the city of Lyon have been obtained from Lidar measurements of atmospheric backscattering, over a period of three days. The concentrations measured at 50 m above the ground have been compared with the mass concentration of PM10 measured by a ground-based sampler located near the Lidar site. At certain times during the measurement campaign, the Lidar concentration measurements at 50 m agree reasonably well with the concentrations at ground level but at other times the differences between the two sets of measurements are so great that they cannot be explained by possible uncertainties in the data processing. Even when the Lidar and ground-based measurements coincide, there are significant differences between the two signals. To explain these differences we have computed the trajectories of the air parcels that pass over the Lidar, using a numerical model for the wind field that takes into account surface features such as relief and changes in roughness. This analysis showed that the differences can be explained by the meteorological conditions (wind speed and direction, vertical profiles of temperature) and the positions of the different sources of particulate matter relative to the measurement site. The combination of Lidar, ground-based sampler and air mass trajectory calculations is shown to be a powerful tool for discriminating between different sources of pollution, which could be useful in enforcing an urban air quality policy.

1. Introduction

Atmospheric aerosols are one of the greatest sources of uncertainty in climate change modelling, responsible for direct and indirect radiative forcing (IPCC, 2007). They play an important role in the complex physical and chemical processes involved in the photochemical reactions that affect air quality in polluted areas (Ravishankara, 2005). Recent studies have shown that aggregation and nucleation processes can occur everywhere (Kulmala and Kerminen, 2008) and especially in urban areas, where they contribute to the formation of primary and secondary organic aerosols in both condensation and accumulation modes (Baltensberger et al., 2005; Imhof et al., 2005). Human health is also sensitive to aerosols; ultra fine urban particles are thought to cause health problems due to their small size and their capacity to absorb Poly Aromatic Hydrocarbons (Kwamena et al., 2006). For all these reasons, the study of the emission, transport and transformation of aerosols in the troposphere and especially in the Planetary Boundary Layer (PBL) has become a key issue for atmospheric chemistry, atmospheric surveys and for climate change modelling. Regional scale studies of atmospheric chemistry such as INDOEX (Satheeshl and Ramanathan, 2000), ESCOMPTE (Dobrinski et al., 2007), ESQUIF (Vautard et al., 2003), CHABLAIS (Beniston et al., 1990) have all highlighted the importance of the spatial distribution of atmospheric aerosols in explaining the chemical transformations in the atmosphere. In this context, remote sensing by Lidar can provide valuable information; vertical profiles of the atmosphere with high temporal and spatial resolution provide real-time dynamic visualization of the PBL height and vertical profiles of aerosol density changes, which can be compared with model predictions. However, in order to be useful for pollution monitoring and to provide the data required for the development of emission reduction strategies, it is necessary to develop methods for making quantitative estimates of aerosol concentration in the urban canopy.

This paper describes a method to explain aerosol time and space concentration variations in an urban canopy of a major city (Lyon, France). It is based on associating UV-Lidar measurements performed during a winter smog episode with measurements from a ground-based sampler close to the Lidar; the differences between

* Corresponding author. Tel.: +33 (0) 472 448 176; fax: +33 (0) 472 431 507.
E-mail address: rairoux@lasim.univ-lyon1.fr (P. Rairoux).

1352-2310/$ – see front matter © 2009 Elsevier Ltd. All rights reserved.
doi:10.1016/j.atmosenv.2009.12.031

the two data sets are investigated using vertical profiles of air temperature, data for traffic flows in the agglomeration and a numerical model to compute the trajectories of the air masses passing over the measurement site. Although the measurements that form the basis of this paper were made in 2002, we believe that the results remain relevant, and the combination of techniques that we have employed here should be useful in future studies.

The paper is organized as follows: we first describe our methodology, based on combining several standard instruments and a commercial numerical dispersion model. We then analyze the Lidar data and explain how we obtain the aerosol mass concentration distribution. The paper ends with a combined analysis of the Lidar data, the trajectory calculations, and the ground-based PM10 measurements which demonstrates how this combined approach can be used to identify and discriminate between different sources of pollution. The thermal stability of the atmosphere is shown to play an important role in determining the differences between what is measured at the ground and what is measured higher up, by the Lidar.

2. Methodology

Lidar vertical profiles of aerosol mass concentration show strong diurnal variations that are not directly linked to variations in meteorological conditions. To explain these variations, we have computed the trajectories of the air masses that pass through the measuring volume of the Lidar at each instant, and we have used ground-based measurements of traffic flows and PM10 concentrations to provide a qualitative indicator of the temporal variation in the aerosol mass load of the air passing through the measuring volume.

2.1. Geographical situation

Lyon is located at the upper end of the Rhône valley where the wind blows mainly from the SouthWest. Substantial hills to the North (Croix-Rousse) and West (Fourvière) of the city centre influence air flow over the city; the terrain to the East and the South is relatively flat and homogeneous. The main sources of aerosols are the chemical plants located to the South of the city, domestic heating and vehicle emissions. Air quality in the city is measured by the COPARLY[1], and we have used data from two of their samplers to supplement and explain the profiles measured by the Lidar:

- La Mulatière, to the South of the city, close to the Lyon-Marseille motorway, which provides a good indication of traffic flow through the city,
- Croix-Luizet, to the North East of the city, which provides a good indication of traffic emissions in the immediate vicinity of the Lidar site;

These stations provide hourly-averaged values of PM10 dry particle concentrations at ground level, measured using the TEOM technique. These different locations are indicated in Fig. 1, together with major topographical features and the main road network. In most normal meteorological conditions, PM2.5 concentrations are correlated with traffic emissions rather than PM10 (Gomes et al., 2008), but PM10 remains a useful indicator of pollutant emissions from traffic flows (Vester et al., 2007). Moreover, PM2.5 was not available during our 2002 study. Vehicle traffic on the inner ring road was measured using a counter located at Vaulx-en-Velin, which supplied hourly-averaged traffic flow data. The Lidar was located on the campus of the Lyon University, to the North East of the city. Meteorological data (wind speed and vertical profiles of temperature and humidity) were supplied by Météo France from measurements made at Bron. Measurements at the Lidar site should not be too different from those measured at Bron, because of the relatively flat and homogeneous terrain between these two sites. The simulations of the trajectories of the air masses passing over the Lidar site were made using hourly measurements of wind velocity at Solaize, to the South of the city.

2.2. Meteorological conditions

During the whole measurement period, the weather conditions remained relatively settled with a light wind (wind speeds in the range 0.5–1 m s^{-1}) blowing from the SouthWest (wind direction generally around 210°); the data are shown in Fig. 2. The very rapid and short-lived changes in wind direction on January 11th and January 13th are not significant, since they occurred at times of very light winds, but on the 12th January the wind changed direction, and blew steadily from the North East, at a speed of about 0.4 m s^{-1}, for a period of about 7 h, before reverting to its original direction.

Vertical profiles of temperature and humidity were measured four times a day by Météo France at the airport at Bron; these profiles are shown in Fig. 3. The profiles show similar behaviour over the three days of this study; the lower part of the atmosphere is very stable at night and in the early morning, with a temperature inversion around 400 m, and a nearly adiabatic profile above 400 m. By around midday each day, heating from the ground has inverted the temperature gradient, creating a slightly convective layer which extends up to about 400 m, capped by a thin layer of stable air.

The Relative Humidity (RH) varied in a similar way over the period of the study. Close to the ground, it rises to 90–100% during the night and early morning, falling to about 55–70% during the day; these diurnal variations in RH extend up to about 100 m from the ground, and it is only above this height that the values tend to become relatively steady over the day. For most of the time, the RH in the PBL remained below 70% and this has a significant impact on the hygroscopic growth of aerosol particles.

2.3. Ground-based measurements of traffic flows and PM10

Fig. 4 shows the traffic flows on the inner ring road, in vehicles per hour, together with PM10 mass concentration measured at La Mulatière and at Croix-Luizet. The volume backscattering *R*-ratio for the Lidar (see Section 2.5) is also shown on the graph, for comparison, at a height of 50 m. The Lidar did not provide an unbroken record during the measurement period, so there are gaps in the *R*-ratio curve, corresponding to the periods without a Lidar signal.

The traffic flow measured at Vaulx-en-Velin shows two peaks on the 11th January, corresponding to rush hours, and single, broader peaks on the 12th and 13th January, reflecting the general change in vehicle usage over the weekend. It represents traffic flows within the agglomeration. PM10 mass concentrations measured at La Mulatière and at Croix-Luizet are in general strongly influenced by traffic flows, since both stations are close to major traffic arteries and motorways. The station at La Mulatière is also exposed to emissions from the chemical plants to the South, when they are carried northwards over Lyon by the wind. In general, PM10 concentrations are highest during the day, and lowest at night, and this coincides with variations in traffic flows measured at Vaulx-en-Velin. The concentrations are higher on the 11th January (Friday) than on the following two days because traffic flows are lower at the weekend. The highest PM10 concentration (205 μg m^{-3}) was observed at La Mulatière at around midday on the

[1] Comité pour le contrôle de la Pollution Atmosphérique dans le Rhône et la région Lyonnaise.

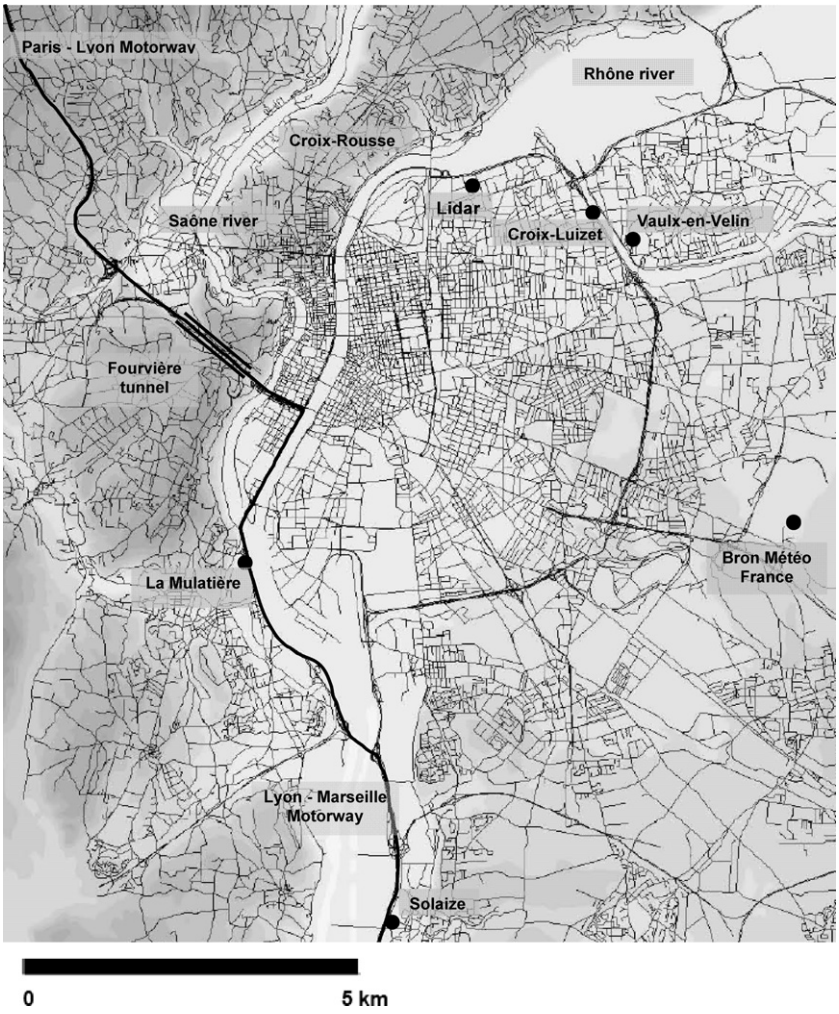

Fig. 1. General geographical situation: the Lidar site is shown together with major topographical features (Croix-Rousse, Fourvière), the main road network (Paris–Lyon motorway, Lyon–Marseille motorway), two PM10 monitoring stations (La Mulatière, Croix-Luizet), a vehicle traffic counter (Vaulx-en-Velin) and meteorological sites (Météo France Bron, Solaize).

11th of January, and this coincides well with the peak measured at Croix-Luizet. The concentrations exceed the regulatory daily average threshold of 50 μg m^{-3} for almost the entire period.

2.4. Lidar measurements

The Lidar consists of a 10 ns pulsed Nd:YAG laser source emitting at 355 nm to ensure eye-safety, combined with an f/3 (200 mm aperture) Newtonian telescope to collect backscattered light from the atmosphere. A 3 nm interference filter inserted on the detector optical path ensures daylight suppression, and photoelectrons are recorded using a 40 MHz 10-bit transient recorder (Licel) providing 7.5 m range-resolution. Vertical profiles are measured over a period of 30 s, and successive profiles are averaged over a period of 15 min. The Lidar signal results from backscattering and extinction of atmospheric aerosols and molecules and the aerosol load in the atmosphere can be obtained from the Lidar backscattering *R*-ratio defined at altitude *z* from ground level as (Weitkamp, 2005):

$$R(z) = 1 + \beta_a(z)/\beta_m(z) \quad (1)$$

where β_m (resp. β_a) refers to the molecular (resp. aerosol) volume backscattering coefficient ($R = 1$ corresponds to an aerosol-free atmosphere). The Klett iterative algorithm (Böckmann et al., 2005) was used to compute the Lidar *R*-ratio as a function of *z*-altitude. The starting point z_0 for the inversion algorithm was taken just above the PBL, and the value of *R* at z_0 was determined by the convergence of the Klett inversion algorithm. For this study, $z_0 = 600$ m, and $R(z_0) = 1.20 \pm 0.06$. To apply the Klett inversion algorithm, a predefined value for the *S*-ratio is needed, where the *S*-ratio is defined as the ratio between the optical extinction coefficient α_a and the volume backscattering coefficient β_a of the atmospheric aerosols. The *S*-ratio, which is sensitive to the aerosol microphysics and to the chemical composition of the particles (Anderson et al., 2000), is altitude dependant. For this study, we have used a mean value of 30 which agrees with the values used in similar studies, to within 20% (Mathias and Bösenberg, 2002). The precision of the computed *R*-values is estimated to range from 5% at the top of the PBL to 10% near ground level, R_0 and *S* being the main sources of uncertainty.

Fig. 5 is an example of a Lidar *R*-ratio vertical profile retrieved from the Lidar measurements taken at 16h30 on January 11th. Between 50 m and 170 m the *R*-values fluctuate in the range from 2 to 3.8, due to corresponding fluctuations in particle concentrations. Between 170 m and 300 m the *R*-values are relatively constant, indicating that particles are mixed much more evenly in this part of the atmosphere. These observations can be correlated with vertical profiles of atmospheric temperature (Fig. 3). In the lower part of the atmosphere, up to a height of about 170 m, the temperature decreases with altitude more rapidly than the adiabatic dry lapse

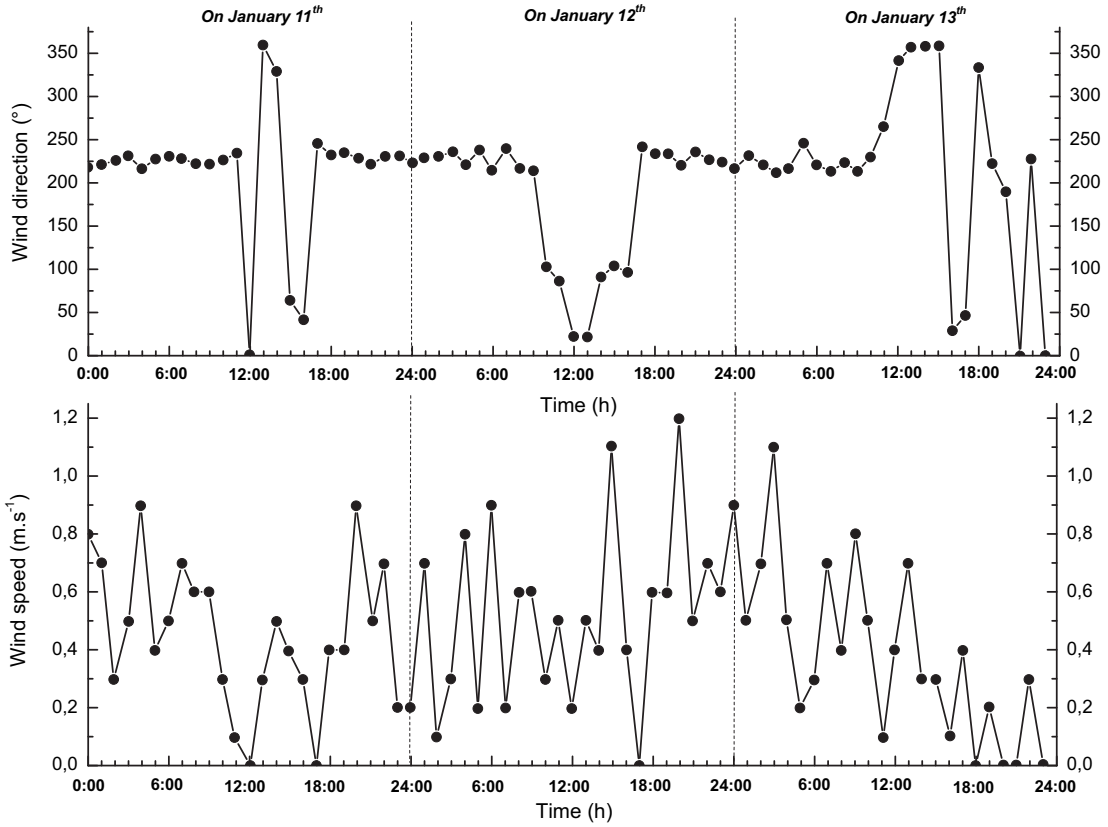

Fig. 2. Wind direction and wind speed measurements made at Bron. On the 12th January, the wind changed direction and blew steadily from the North East.

rate indicating the presence of a convective mixed layer with strong vertical transport of ground-generated aerosols. Between 170 m and 300 m, the temperature decreases with altitude less rapidly than the adiabatic dry lapse rate, suggesting a relatively stable layer, with much reduced vertical mixing. The boundaries of these two regions correspond to the Mixed Layer height and the PBL height, which we have also evaluated directly from the temperature profiles.

Atmospheric humidity can strongly influence particle size, especially for urban aerosol field studies; for values of the Relative Humidity over 70%, the mean size growth factor approaches 1.7, and can rise to 2 close to the deliquescence point (Randriamiarisoa et al., 2006). We account for possible effects of moisture content by correcting the measured values of R to give the equivalent value of R for scattering from dry particles. To do this, we used a recent method (Boyouk et al., 2009) in which the correction coefficient f_{scat} for the optical measurements is given by:

$$f_{scat} = [(1 - RH)/(1 - RH_{ref})]^{y} \quad (2)$$

where RH_{ref} is the reference value for the Relative Humidity, at which the scattering coefficient no longer varies with moisture content and γ is the Hänel coefficient. We have taken $RH_{ref} = 0.6$ and $\gamma = 0.5$ as proposed by Herich et al. (2008) for urban aerosols. Above 50 m, our measured Relative Humidity lies between 55 and 80%, leading to correction coefficient f_{scat} values between 1 and 0.7.

2.5. Aerosol mass concentration retrieval

We then retrieved the aerosol mass concentration M (in $\mu g\ m^{-3}$) from our R-Lidar ratio measurements, using Del Guasta's method (Del Guasta and Marini, 2000), through the following linear relation:

$$M = K\beta_a \quad (3)$$

where β_a (in $cm^{-1}\ sr^{-1}$) is deduced from R-Lidar ratio measurements, by applying equation (1) and optical molecular scattering, using estimates of the vertical distribution of the density deduced from PTU radio soundings (Fig. 3). The K constant stands as a mass coefficient (in $\mu g\ sr\ m^{-2}$), which can be calculated by $K = <m_a>/<d\sigma_a/d\Omega>$, where $<m_a>$ is the mean aerosol mass and $<d\sigma_a/d\Omega>$ is the mean aerosol backscattering cross-section, computed for a predefined aerosol size number density distribution (Fig. 6) and its associated chemical composition. To do this, we have used the available physical and chemical data for dry particles in the urban atmosphere (Malet et al., 2004; Imhof et al., 2005) by assuming a three-mode log-normal particle number density distribution (median diameter D_m, spread s_m and relative concentration C).

The nucleation mode ($D_m = 30$ nm, $s_m = 2$, $C = 0.66$) consists principally of primary soot particles and organic particles produced by the combustion of fossil fuels. These small particles contribute relatively little to the optical scattering signal, but very strongly to optical absorption. Only soot particles have been considered and modelled by Rayleigh–Gans scattering theory for diffusion from fractal particles (Schnaiter et al., 2003).

The accumulation mode ($D_m = 90$ nm, $s_m = 1.8$, $C = 0.33$), composed of secondary particles, is assumed to be an internal mixture (by volume, soot and sulphate aggregates: 60%, organic matter: 40%) (Worringen et al., 2008; Vester et al., 2007). These particles, assumed to be spherical to apply Mie theory, dominate optical scattering by the aerosol in the UV spectral range.

The coarse mode ($D_m = 2000$ nm, $s_m = 1.7$, $C = 10^{-5}$) is assumed to be composed of an internal mixture (by volume, silicates: 50%, soot particles agglomerates: 50%) (Vester et al., 2007). Salt was not included because our stable atmospheric conditions severely limit the proportion of marine air in the mixed urban layer. For these

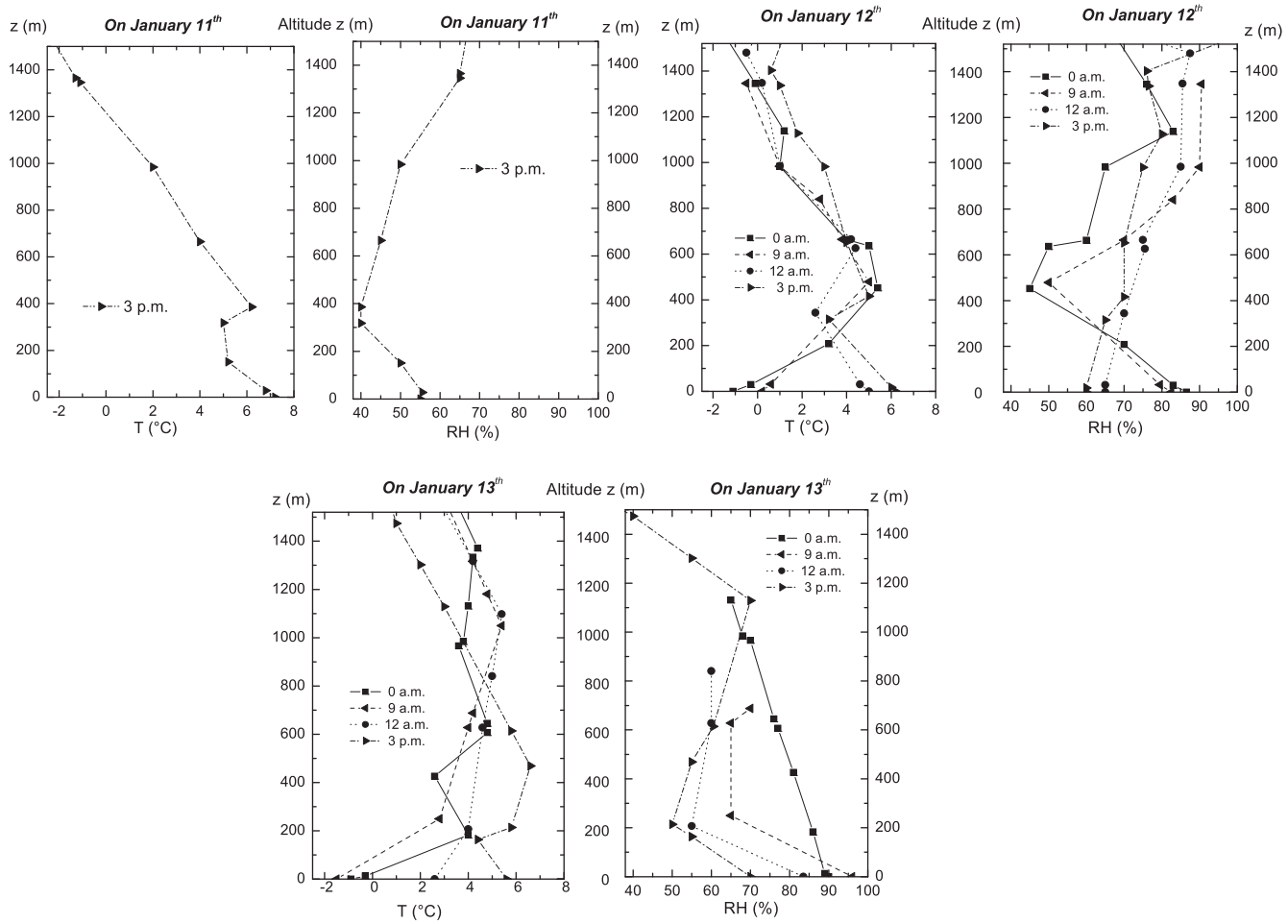

Fig. 3. Vertical profiles of temperature T (°C) and relative humidity RH (%) measured by Météo France at Bron from the 11th January to the 13th January.

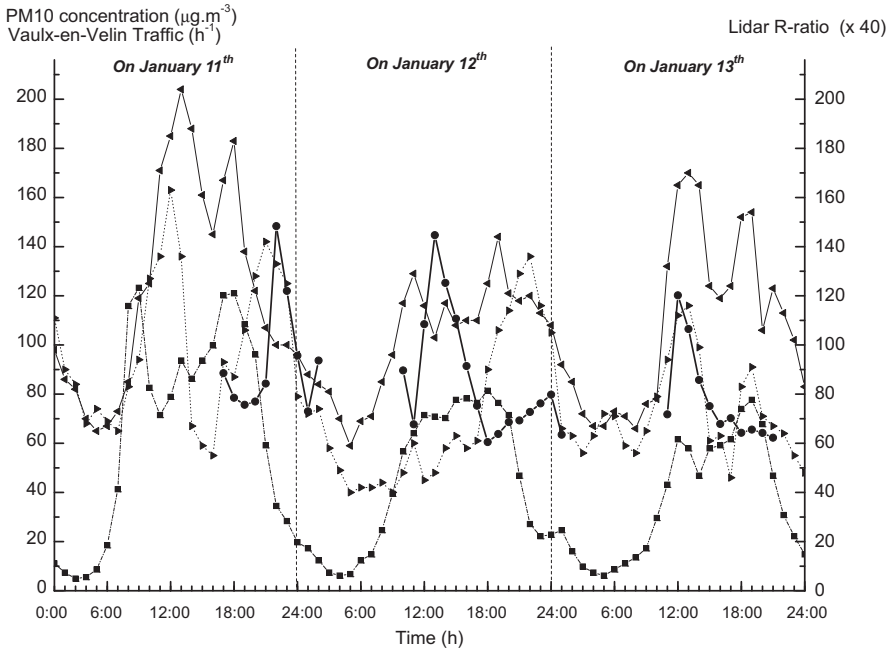

Fig. 4. Temporal evolution of PM10 mass concentration at La Mulatière (left triangle) and at Croix-Luizet station (right triangle), vehicle flows at Vaulx-en-Velin (squares) and Lidar backscattering R-ratio at La Doua, at an altitude of 50 m (circles). The Vaulx-en-Velin vehicle traffic counter (resp. the Lidar R-ratio) has been multiplied by 100 (resp. 40) to make the graph clearer.

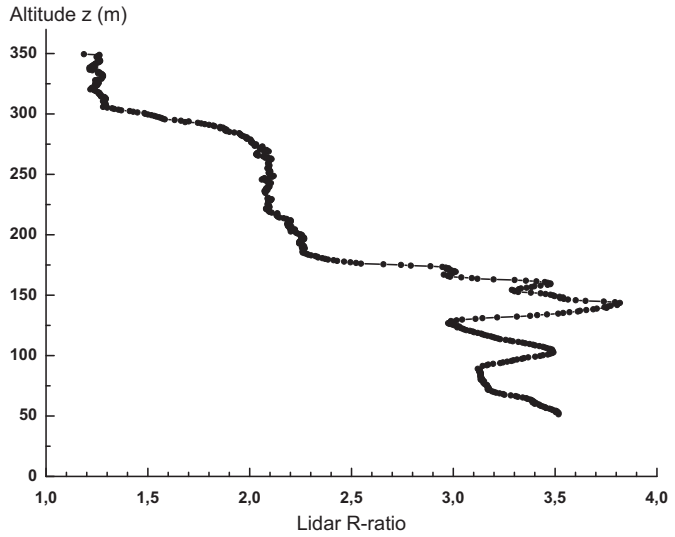

Fig. 5. Vertical profile of the Lidar backscattering ratio *R*, monitored on the 11th January at 16 h 30. Measurements below 50 m are not achievable with the Lidar optical setup.

aged particles, Mie scattering theory was applied (Del Guasta, 2002). Their relatively low number (Gomes et al., 2008) limits their contribution to optical scattering, even though they contribute 25% of the total mass of particles (Nicolas et al., 2009).

We calculated the refractive index by applying the volume-mixing rule for externally mixed particles proposed by Worringen et al. (2008), using 355 nm-refractive index and densities given in Table 1. We thus obtain $K = 4.2 \times 10^6$ μg sr m^{-2} with an uncertainty of the order of 30%, related to the aerosol chemical composition, relative concentrations of the different components. This leads to a 40% uncertainty in *M*, which indicates that comparison with ground-based PM10 concentration measurements will be limited to high aerosol concentrations.

2.6. Local air parcel trajectories

To evaluate the origin and the evolution of the air passing over the Lidar station, numerical simulations of air particle trajectories have been performed using the numerical model FLOWSTAR (Hunt et al., 1988) which is included as part of the ADMS-3 model (Futter, 2000). The model calculates a steady wind field, from a Fourier transform solution of the linearized equations of motion, taking account of orographic effects, provided that the terrain is not too steep. It also includes the influence of atmospheric stability through the use of Monin–Obukhov similarity theory (Irwin and Binkowski, 1981). The boundary conditions for the model are therefore the ground elevation in the calculation domain, the variation in roughness height within the domain, the surface heat flux and a wind velocity at a reference height, at one point in the domain. The model has been used to compute the flow in a domain measuring 32 km × 32 km which includes all of the city of Lyon and the hilly relief to the North and the West. The wind field was computed using the hourly measurements of wind speed and direction from a meteorological station located at Solaize, to the South of the city (see Fig. 1); this therefore provided a set of 72 steady wind fields for the duration of the experiment. We have assumed that the wind speed and direction varied linearly between these hourly measurements, so the wind field at any intermediate time can be obtained by a linear interpolation between the two computed fields. Forward and backward trajectories of air masses passing 50 m above the Lidar station have thus been calculated using an Eulerian advection scheme, with a 1 min time step.

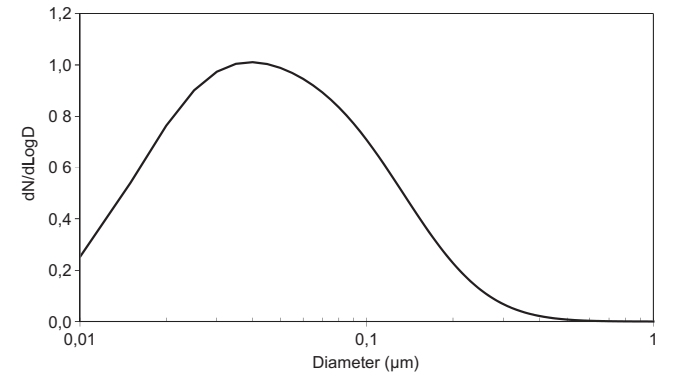

Fig. 6. Urban number aerosol size distribution used for aerosol mass concentration retrieval from Lidar backscattering measurements.

Table 1
Aerosol particles 355 nm-refractive index and density to be considered in the calculation of *K*-mass coefficient.

Aerosol mode	355 nm − refractive index	Density (g cm^{-3})
Nucleation mode		
Soot	1.4 + 0.64i (Schnaiter et al., 2003)	1.0 (Schnaiter et al., 2003)
Accumulation mode		
Organics	1.638 + 0.01 (Dinar et al., 2008)	1.3 (Mallet et al., 2004)
Mixed soot-sulphate	1.53 + 0,05i (Worringen et al., 2008)	1.6 (Vester et al., 2007)
Coarse mode		
Silicate	1.55 + 0i	2.6
Soot aggregate	1.5 + 0.5i (Kasparian et al., 1998)	1.0 (Schnaiter et al., 2003)

3. Results and discussion

Vertical profiles of aerosol concentration measured by the Lidar have been plotted as a function of time in Fig. 7. The white-coloured areas on January 13th at 12h00 and 20h00 correspond to the presence of low altitude cloud which prevented the computation of aerosol concentrations. The heights of the PBL and the mixed layer are visualised by the change in colour from purple to dark blue and from dark blue to light blue respectively; a comparison with the *R* profile in Fig. 5, for 16h30 on the 11th January, shows that these two rather sharp colour transitions correspond to the two heights (170 m and 280 m) at which the *R*-ratio varies rapidly with altitude.

The highest concentrations occur closest to the ground, indicating that the aerosol load is dominated by the contribution from ground-level emissions upwind of the Lidar. This is confirmed by the fact that the particle concentrations vary more rapidly at higher altitudes; the emissions vary on a rather long timescale, whereas the concentrations at higher altitudes are determined by unsteady convective motions in the boundary layer, with much shorter time scales. The temperature profiles (Fig. 3) show that the regions of high particle concentration penetrate further into the atmosphere when the lower boundary layer is convective.

The peak particle mass concentration computed from the Lidar measurements on the 11th January (at 21h00 and an altitude of 50 m) agrees rather well with the ground-level concentration measured at the same time – 120 μg m^{-3} for the Lidar data, compared with 140 μg m^{-3} for the ground-based measurement. The difference between the two can easily be accounted for by the

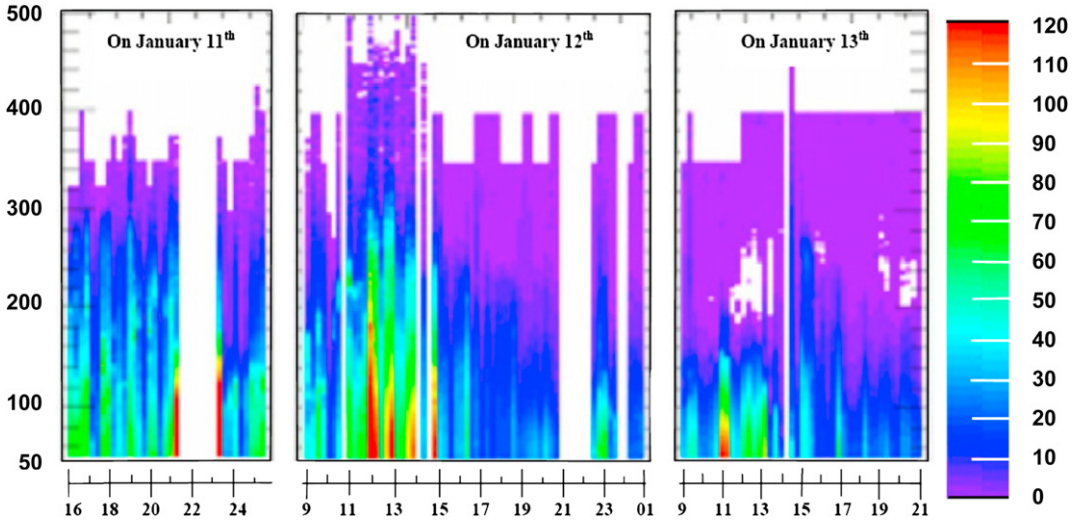

Fig. 7. Time and range resolved distribution of urban aerosol mass concentration. The colour scale from purple to red gives the aerosol concentration, expressed in μg m^{-3}, while the white sections represent missing measurement periods during night-time.

effects of convection and dilution, and by uncertainties in the computation of mass concentrations from the Lidar measurements.

During the nights of the 12th and 13th January the particle concentrations above 50 m are very much reduced compared with the daytime values, which can probably be explained by the strong stratification of the boundary layer (Fig. 3) coupled with a reduction in vehicle emissions – as can be inferred from the traffic flows at Croix-Luizet, (Fig. 4).

The ground-level concentrations at Croix-Luizet also decrease during the periods 0h00–10h00 and 0h00–08h00 on the 12th and 13th January respectively. This suggests that the Lidar concentrations decrease because of a drop in emissions, rather than because of strong stratification close to the ground, since this would tend to increase ground-level concentrations through the trapping of particles.

The Lidar measurements and those at Croix-Luizet do not always agree so well, as can be seen from Fig. 3. Although this graph shows the *R*-ratio, rather than the concentrations, the plot has been scaled so that it is close to the equivalent particle mass concentration. The *R*-ratio at 50 m agrees reasonably well with the ground-based data for the 11th and 13th January, but the two are very different on the 12th January, most notably in that the Lidar data show a peak at 13h00, whereas the ground-based measurements show a peak of similar magnitude, at 22h00.

To understand the differences between the two, we have computed the trajectories of the air parcels that pass over the Lidar measurement site, as described in Section 2.6; three such trajectories have been plotted in Fig. 8, corresponding to the air masses that generate the peak concentrations 50 m above the Lidar, for each of the three days of this study.

On the evening of 11th January the wind blew fairly steadily from the SouthWest, so the air sampled by both the Lidar and the sampler at Croix-Luizet will have passed over the city centre, and over the Lyon-Marseille motorway taking about an hour, the measurements represent an integral of all that was emitted by the agglomeration during the preceding hour. It is not surprising, therefore that the peak concentrations at the two sites occur at the simultaneously (Fig. 4), towards the end of the evening rush hour; several hours after the maximum traffic flow for the evening rush hour. However, the concentrations increase at very different rates – the ground-level concentrations increases fairly steadily over the period 16h00–21h00, corresponding to the build-up of traffic in the evening rush hour, whereas at 50 m the concentration increases much more rapidly between 20h00 and 22h00. Fig. 7 shows that this rapid rise corresponds to a very sharp spatial concentration gradient; very rapidly, the region of high particle concentration rises up to a height of 120–130 m, and drops at a similar rate later in the evening. Upwards vertical diffusion is unlikely to be able to account for such sharp gradients, nor for such deep mixing, even if the city acts as a heat island, driving convection in the boundary layer. A possible explanation is that the air parcels will have passed over the tunnel under Fourvière at the height of the evening rush hour, when there is always a tailback, several kilometres long, on both sides of the tunnel. The polluted air in the tunnel – which is also much warmer than the atmospheric air – is discharged to the atmosphere through chimneys at each end of the tunnel and rises in the atmosphere driven by the temperature difference and momentum. Urban emissions, however, remain confined to the lower layers of the atmosphere by the thermal stratification in the boundary layer, and this determines the broader peak measured at Croix-Luizet.

On January 13th the peaks in the Lidar and ground-level concentrations at Croix-Luizet again coincide. As on the 11th January, the region of high concentration detected by the Lidar is defined by very sharp concentration gradients in space and in time, with rapid, deep penetration into the upper layers of the urban boundary layer. The ground-based measurement shows a slower increase in concentration, but the two systems give broadly similar values for the maximum concentration. The peak concentration coincides with a peak in the traffic flow measured at Vaulx-en-Velin. The major difference with the conditions on the 11th January is that initially the wind blows from the SouthWest, but then changes direction, between 11h00 and 12h00, from which time onwards it blows from the North. As a result the air masses that are measured at midday over the Lidar and at Croix-Luizet, have not passed over the city centre, nor over the tunnel under Fourvière and will have encountered very little pollution in their immediate past (Fig. 8). As for the 11th January, the form of the region of high concentration in the Lidar measurements is characteristic of a concentrated emission from a point source and the most likely explanation for this peak is the ventilation system on the Northern part of the ring road (TEO) which is entirely in tunnel, and which leads directly to the traffic counting station at Vaulx-en-Velin. Later on, in the early evening of the 13th January there is a second peak in

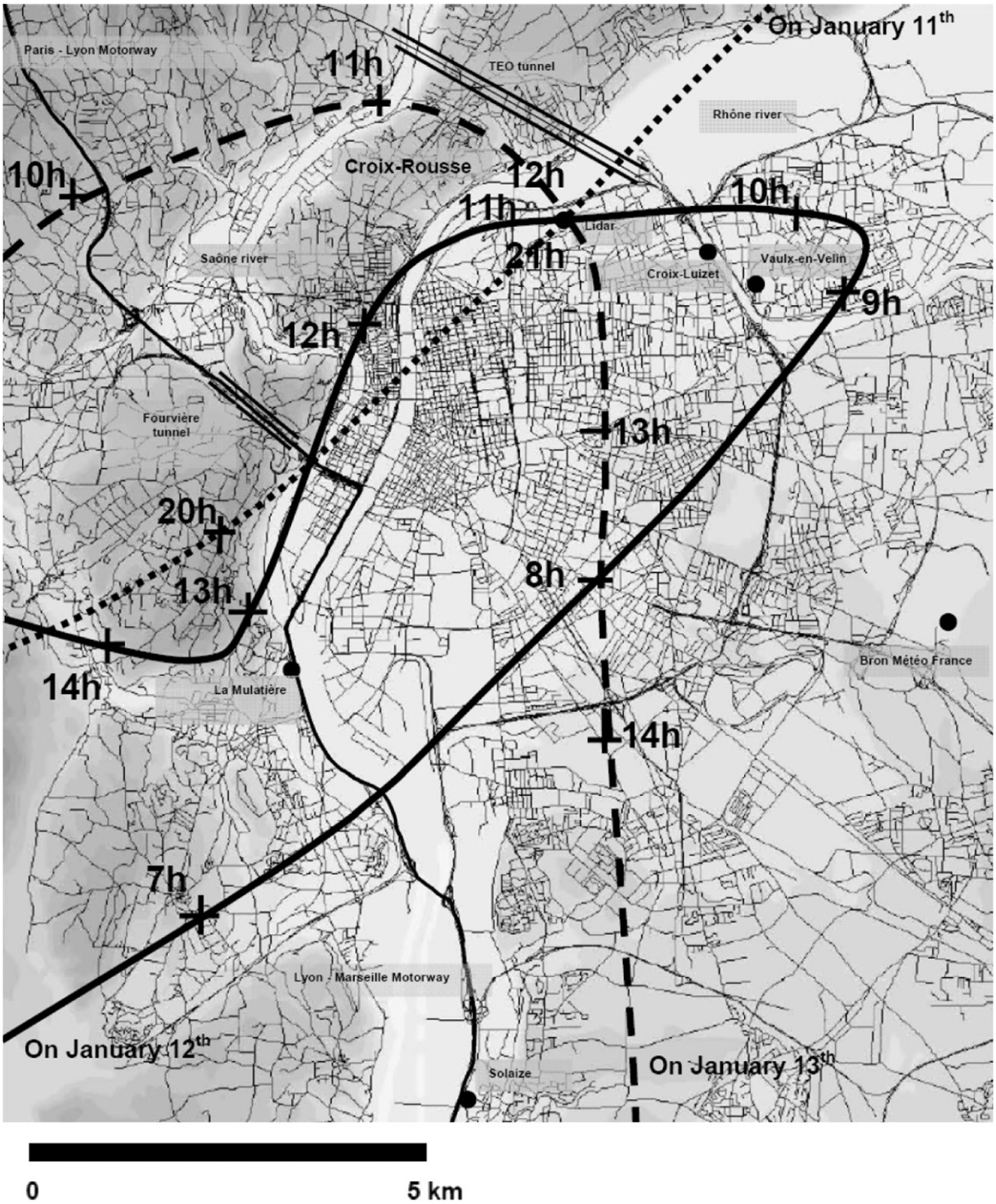

Fig. 8. Local air parcel trajectories computed using FLOWSTAR (ADMS-3), for the three Lidar measurements days: 11th January (dot line), 12th January (solid line), 13th January (dash line).

the ground-level concentrations which coincides with a smaller peak in the traffic flow but which does not figure at all in the concentrations measured by the Lidar. This is probably explained by the fact that the emissions from traffic on the ring road are detected by the ground-based sampler, but they are prevented from diffusing upwards by the thermal stability of the boundary layer (see Fig. 3) so they are not detected above 50 m.

The data for the 12th January are quite different The Lidar records a significant peak between 12h00 and 13h00, whereas ground-level concentrations only rise to comparable levels later in the evening (19h00–24h00). The trajectory plot (Fig. 8) shows that the wind changed direction several times during the day; early in the morning the wind blew from the SouthWest, beginning to change direction at about 10h00, blowing first from the East before settling down to blow from the North. At about 14h00 it began to rotate back, blowing first from the East and finally stabilising at around 18h00 to blow once again from the SouthWest (Figs. 2 and 8). The air that passes over the Lidar site at 11h00 has therefore

passed over the Lyon-Marseille motorway at around 07h00 and then over the whole of the city. Because of the changes in wind direction, the air masses that passed over the Lidar at 12h00 and 13h00 will have had similar trajectories, but shifted eastwards by 2–3 km. These trajectories will have passed over the petrochemical refineries at St. Fons and Solaize at around 07h00 in the morning. It is therefore likely that the strong vertical plumes that are measured by the Lidar are the result of emissions collected during the passage over Solaize and St Fons. The plumes are more diffuse than those from the tunnels because the travel time between source and Lidar are much longer. These industrial plumes do not appear to have been detected at Croix-Luizet, where the concentrations are entirely consistent with the traffic flows measured at Vaulx-en-Velin. Previous studies of gaseous pollutant dispersion over Lyon (Soulhac et al., 2003) using nested models and a source inventory showed that the ground-level concentrations in the North Eastern part of the city were dominated by vehicle and domestic emissions, and were relatively independent of industrial emissions to the South of the city. The broad peak in the measured concentrations at Croix-Luizet between 18h00 and 24h00 occurs when the wind is once again blowing from the SouthWest (Fig. 2), bringing air over the city before it encounters the sampler. Vertical diffusion of the polluted air is limited by the thermal stratification of the atmosphere (Fig. 3) so the Lidar only records a rather broad, diffuse increase in the concentrations above 50 m.

4. Conclusions and further work

Vertical profiles of particle mass concentration have been obtained from Lidar measurements of atmospheric backscattering, over a period of three days, and the concentrations measured at 50 m above the ground have been compared with the mass concentration of PM10 measured by a ground-based sampler located reasonably close to the Lidar site. For optical reasons, it was not possible to make Lidar measurements closer to the ground. In order to obtain mass concentrations from the optical backscattering it was necessary to make a number of assumptions about the atmospheric aerosol, and it is estimated that this leads to an uncertainty of about 40% in the computation of the mass concentration. For certain periods during the measurement campaign, the Lidar concentration measurements at 50 m agree reasonably well with the concentrations at ground level – the differences between the two are easily within the estimated error bounds for the computation of concentrations from the measured backscattering. At other times the differences between the two sets of measurements are so great that they cannot be explained by possible uncertainties in the data processing. Even when the Lidar and ground-based measurements coincide, there are significant differences between the two signals. In order to explain these differences it is necessary to consider the trajectories of the air masses that pass over the measurement stations; we have computed these trajectories using a numerical model for the wind field that takes into account surface features such as relief and changes in roughness. This analysis showed that the differences can be explained by the meteorological conditions (wind speed and direction, vertical profiles of temperature) and the positions of the different sources of particulate matter relative to the measurement site. As a general conclusion, the ground-based sampler is strongly influenced by emissions in the immediate vicinity, and, in particular, by vehicle emissions. On the other hand, the most marked peaks in the Lidar measurements are caused by plumes of pollutant that penetrate much further into the upper layers of the boundary layer, and seem to be generated by point sources linked either to tunnel ventilation or to petrochemical plants. The thermal stratification of the atmosphere acts to separate the influence of these phenomena. The comparative lack of influence of these point sources on the concentrations measured by the ground-based sampler confirms the results of an earlier numerical study which examined the dispersion of pollutants in the urban canopy over Lyon (Soulhac et al., 2003). It therefore follows from this that the data from ground-based samplers, taken in isolation, can give a very misleading picture of particulate concentrations in the urban canopy, and that vertical profiles of the type provided by a Lidar can reveal significant quantities of material that are not detected at ground level. Coupling the Lidar profiles with a trajectory model provides a powerful tool for source identification, which could prove invaluable in enforcing an air quality policy.

The accuracy of the mass concentration estimates could improve measurements based on elastic and inelastic multi-wavelength Raman scattering (Pappalardo et al., 2004). The accuracy will also be improved by including microphysical properties of the aerosols (such as their hygroscopic properties). More detailed numerical modelling should enable a better discrimination between sources, and the inclusion of source terms and dispersion calculations would make it possible to compare the measured concentrations with those predicted by the model. Detailed modelling of the flow and dispersion in the neighbourhood of the ground-based sampler, as described in Soulhac et al. (2008) should help in determining the relative contributions of local emissions (traffic, domestic heating…) and more distant point sources. The results from this study will be used in the planning of a larger, more comprehensive measurement campaign, which will investigate, in particular, the interaction between the complicated structure of the urban canopy and the emissions from point sources outside the agglomeration.

Acknowledgements

We would like to thank COPARLY, Météo France, Bron and the DDE Rhône Alpes for supplying the pollution, meteorological and traffic data used in this study. The work was part-funded by ADEME and the Région Rhône-Alpes. We gratefully acknowledge the assistance of F. Dugay and F. Nicolas-Guizon in analyzing some of the data.

References

Anderson, T.L., Masonis, S.J., Covert, D.S., Chalrson, R.J., Rood, M.J., 2000. In situ measurement of the aerosol extinction-to-backscatter ratio at a polluted continental site. J. Geophys. Res. Atmos. 105 (D22), 26907–26915.

Baltensberger, U., et al., 2005. Secondary organic aerosols from anthrogenic and biogenic precursors. Faraday Discuss. 130, 265–278.

Beniston, M., Wolf, J.P., Beniston-Rebetez, M., Kölsch, H.J., Rairoux, P., Wöeste, L., 1990. Use of Lidar measurement and numerical model in air pollution research. J. Geophys. Res. 95 (D7), 9879–9894.

Böckmann, C., et al., 2005. Aerosol lidar intercomparison in the framework of the EARLINET project. 2. Aerosol backscattering algorithms. Appl. Opt. 43 (4), 977–989.

Boyouk, N., Léon, F.F., Delbarre, H., Podvin, T., Deroo, C., 2009. Impact of the mixing boundary layer on the relationship between PM2.5 and aerosol optical thickness. Atmos. Environ.. doi:10.1016/j.atmosenv.2009.06.053.

Del Guasta, M., Marini, S., 2000. On the retrieval of urban aerosol mass concentration by a 532 nm and 1064 nm Lidar. J. Aerosol Sci. 12, 1469–1488.

Del Guasta, M., 2002. Daily cycles in urban aerosols observed in Florence (Italy) by means of an automatic 532–1064 nm LIDAR. Atmos. Environ. 36, 2853–2865.

Dinar, E., Abo Riziq, A., Spindler, C., Erlick, C., Kiss, G., Rudich, Y., 2008. The complex refractive index of atmospheric and model humic-like substance (HULIS) retrieved by cavity ring down aerosol spectrometer. Faraday Discuss. 137, 279–295.

Dobrinski, P., et al., 2007. Regional transport and dilution during high-pollution episodes in southern France: summary of findings from the field experiment to constraint models of atmospheric pollution and emissions transport, (ESCOMPTE). J. Geophys. Res. Atmos. 112 (D13), D13105.

Futter, D.N., 2000. Comparison of monitored air quality data with the predictions of ADMS-3. Adv. Air Pollut. Ser. 8, 515–528.

Gomes, L., Mallet, M., Roger, J.C., Dubuisson, P., 2008. Effects of the physical and optical properties of urban aerosols measured during the CAPITOUL summer campaign on the local direct radiative forcing. Meteorol. Atmos. Phys. 102, 289–306.

Herich, H., Kammermann, L., Weingartner, E., Baltensberger, U., Lohmann, U., Cziczo, D.J., 2008. In situ determination of atmospheric composition as a function of hygroscopic growth. J. Geophys. Res. 113, D16213.
Hunt, J.C.R., Leibowich, S., Richards, K.J., 1988. Turbulent shear flow over hills. Quart. J. R. Met. Soc. 114, 1435–1470.
Imhof, D., Weingartner, E., Ordez, C., Gehrig, R., Hill, M., Buchmann, B., Baltensberger, U., 2005. Environ. Sci. Technol. 39 (21), 8341–8350. doi:10.1021/es048925s.
IPCC, 2007. Fifth Assessment Report. Cambridge University Press, Cambridge, UK and New York, NY, USA, ISBN 978 0521 88009-1.
Irwin, John S., Binkowski, F.S., 1981. Estimation of the Monin–Obukhov scaling length using on-site instrumentation. Atmos. Environ. 15 (6), 1091–1094.
Kasparian, J.F.E., Rambaldi, P., Yu, J., Vezin, B., Wolf, J.P., 1998. Characterization of urban aerosols using SEM-microscopy, X-ray-analysis and Lidar measurement. Atmos. Environ. 32 (17), 2957–2967.
Kulmala, M., Kerminen, V.-M., 2008. On the formation and growth of nanoparticles. J. Atmos. Res. 90, 132–150.
Kwamena, N.O.A., Clarke, J.P., Kahan, T.F., Diamond, M.L., Donaldson, D.J., 2006. Assessing the importance of heterogeneous reactions of polycyclic aromatic hydrocarbons in the urban atmosphere using the Multimedia Urban Model. Atmos. Environ. 4 (1), 37–50. doi:10.1016/j.atmosenv.2006.08.016.
Mallet, M., Roger, J.C., Despiau, S., Putaud, J.P., Dubovik, O., 2004. A study of the mixing state of black carbon in urban zone. J. Geophys. Res. 109, D04202. doi:10.1029/2003JD003940.
Mathias, V., Bösenberg, J., 2002. Aerosol climatology for the planetary boundary layer derived from regular lidar measurements. Atmos. Res. 63, 221–245.
Nicolas, J.F., Yubero, E., Pastor, C., Crespo, J., Carratalà, A., 2009. Influence of meteorological variability upon mass distribution. Atmos. Res. 94, 330–337.
Pappalardo, G., et al., 2004. Aerosol lidar intercomparison in the framework of the EARLINET project. 3. Raman lidar algorithm for aerosol extinction, backscattering, and lidar ratio. Appl. Opt. 43 (28), 5370–5385.
Randriamiarisoa, H., Chazette, P., Couvert, P., Sanak, J., Mégie, G., 2006. Relative humidity impact on aerosol parameters in Paris suburban area. Atmos. Chem. Phys. 6, 1389–1407.
Ravishankara, A.R., 2005. Chemistry-climate coupling: the importance of chemistry in climate issues. Faraday Discuss. 130, 9–26.
Satheeshl, S.K., Ramanathan, V., 2000. Large differences in tropical aerosol forcing at the top of the atmosphere and Earth's surface. Nature 405, 60–63. May 4.
Schnaiter, M., et al., 2003. UV–VIS–NIR spectral optical properties of soot and soot-containing aerosols. Aerosol Sci. 34, 1421–1444.
Soulhac, L., Perkins, R.J., Salizzoni, P., 2008. Flow in a street-canyon for any external wind direction. Boundary Layer Meteorol. 126 (Issue 3), 365–388.
Soulhac, L., Puel, C., Duclaux, O., Perkins, R.J., 2003. Simulations of atmospheric pollution in Greater Lyon: an example of the use of nested models. Atmos. Environ. 37, 5147–5156.
Vautard, R., et al., 2003. A synthesis of the ESQUIF field campaign. J. Geophys. Res. D17, 8564.
Vester, B.P., Ebert, M., Barnert, E.B., Schneider, J., Kandler, K., Schütz, L., Weinbruch, S., 2007. Composition and mixing state of the urban background aerosol in the Rhein-Main area (Germany). Atmos. Environ. 41, 6102–6115.
Weitkamp, C., 2005. Lidar: Range-resolved Optical Remote Sensing of the Atmosphere Springer Series in Optical Sciences, vol. 102. Springer, ISBN 978-0-387-40075-4.
Worringen, A., Ebert, M., Trautmann, T., Weinbruch, S., Helas, G., 2008. Optical properties of internally mixed ammonium sulfate and soot particles – a study of individual aerosol particles and ambient aerosol populations. Appl. Opt. 47 (21), 3835–3845. doi:10.1364/AO.47.003835.